Holocene forearc block rotation in response to seamount subduction, southeastern Peninsula de Nicoya, Costa Rica

Article *in* Geology · February 2001

DOI: 10.1130/0091-7613(2001)029<0151:hfbrir>2.0.co;2

CITATIONS
80

READS
308

11 authors, including:

Jeff Marshall
California State Polytechnic University
44 PUBLICATIONS **1,230** CITATIONS

SEE PROFILE

Dorothy Merritts
Franklin & Marshall College
101 PUBLICATIONS **5,885** CITATIONS

SEE PROFILE

Natalie Kehrwald
United States Geological Survey
86 PUBLICATIONS **2,694** CITATIONS

SEE PROFILE

Marino Protti
National University of Costa Rica
189 PUBLICATIONS **4,686** CITATIONS

SEE PROFILE

Holocene forearc block rotation in response to seamount subduction, southeastern Península de Nicoya, Costa Rica

Thomas Gardner*
Jeffrey Marshall
Dorothy Merritts
Bhavani Bee
Reed Burgette
Emily Burton
Jennifer Cooke
Natalie Kehrwald
Keck Geology Consortium, Carleton College, Northfield, Minnesota 55057, USA

Marino Protti — Observatorio Vulcanológico y Sismológico de Costa Rica, Apartado 86-3000, Universidad Nacional, Heredia, Costa Rica

Donald Fisher
Peter Sak
Department of Geosciences, Pennsylvania State University, University Park, Pennsylvania 16802, USA

ABSTRACT

The southeastern tip of the Península de Nicoya, Costa Rica, on the Caribbean plate margin lies inboard of the rough bathymetric terrain on the subducting Cocos plate and along the landward projection of the convergence vector for the Fisher seamount group. The southern tip of the peninsula has nearly orthogonal coastlines and extensive, well-preserved, Holocene marine terraces, and is ideally situated to evaluate the spatial distribution of forearc deformation in response to seamount subduction.

Two marine terraces that yielded 35 radiocarbon dates give information on the rates, style, and timing of deformation along 40 km of coastline. Ages range from 3.5 to 7.4 ka for a higher terrace and from 0.3 to 2.9 ka for a lower terrace. A maximum uplift rate is ~6.0 m/k.y. along the southeastern tip of the peninsula. Uplift rates decrease linearly to <1.0 m/k.y. along both orthogonal coastlines and thus landward from the Middle America Trench and away from the line of subducting seamounts. The ~400 km^2 region along the tip of the peninsula can be approximated as a rotating block with an angular rotation rate of 0.02°/k.y. about an axis with an azimuth of 80°. Given the modern elevation and dip of the late Quaternary Cobano surface, this style of deformation is limited to a duration of 100–200 k.y. Deformation is occurring in response to seamount bypass or underplating onto the Caribbean plate margin.

Keywords: Costa Rica, marine terrace, Quaternary, tectonism, seamounts.

*Current address: Department of Geosciences, Trinity University, 715 Stadium Drive, San Antonio, Texas 78212; e-mail: tgardner@trinity.edu.

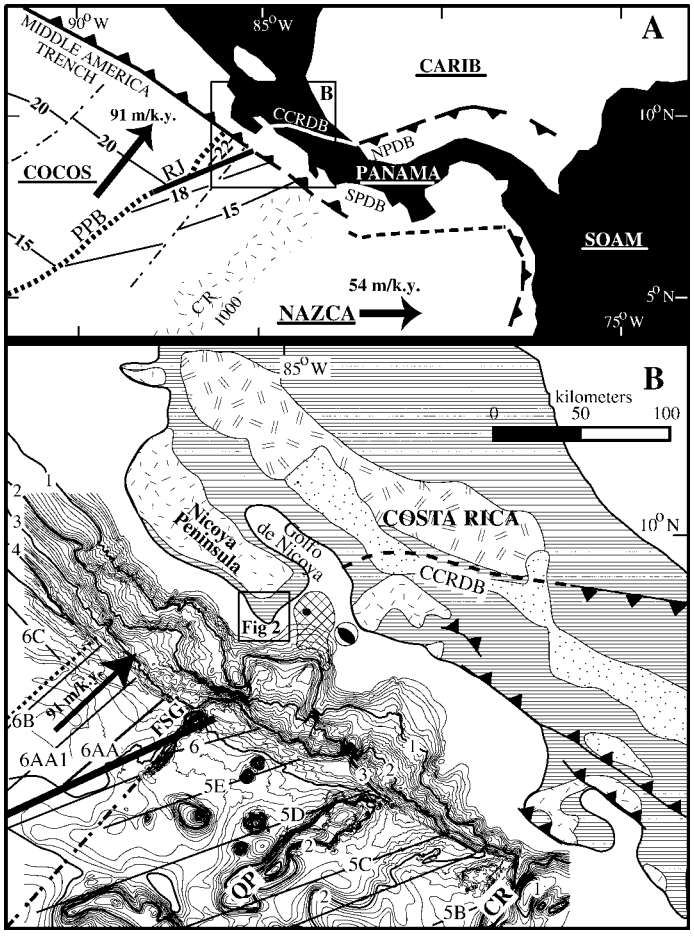

Figure 1. A: Major plate tectonic features of Central America. Names of principle plates are in bold and underlined. SOAM—South America, CARIB—Caribbean, SPDB—South Panama deformed belt, NPDB—North Panama deformed belt, CCRDB—Central Costa Rica deformed belt, PPB—paleoplate boundary, RJ—ridge jump. Inset shows location of B. Major tectonic features are compiled from Mackay and Moore (1990), Silver et al. (1990), Meschede et al. (1998), Barckhausen et al. (2000), and Marshall et al. (2000). Modern plate motion relative to Caribbean is from DeMets et al. (1990) and Protti et al. (1995). Small numbers give age of Cocos seafloor. B: Generalized geologic map of Costa Rica, bathymetry of Cocos plate and location of study area on Península de Nicoya (inset). FSG, Fisher seamount group; QP, Quepos Plateau; CR, Cocos Ridge. Geologic units: Nicoya Complex, random dash pattern; active arc volcanic rocks, random double-dash pattern; extinct-arc volcanic rocks, stipple pattern; Cretaceous and Cenozoic fluvial to marine clastic and volcaniclastic rocks, horizontal line pattern. Bathymetric data are from von Huene and Fluh (1994). Magnetic anomolies are from Barckhausen et al. (2000). Contour interval is 100 m, bold, and labeled every 1 km. Black dot with surrounding hachured area shows epicenter and aftershock extent of March 25, 1990, Golfo de Nicoya subduction earthquake (Mw = 7.0, depth = 20 km) and associated focal mechanism (Protti et al., 1995).

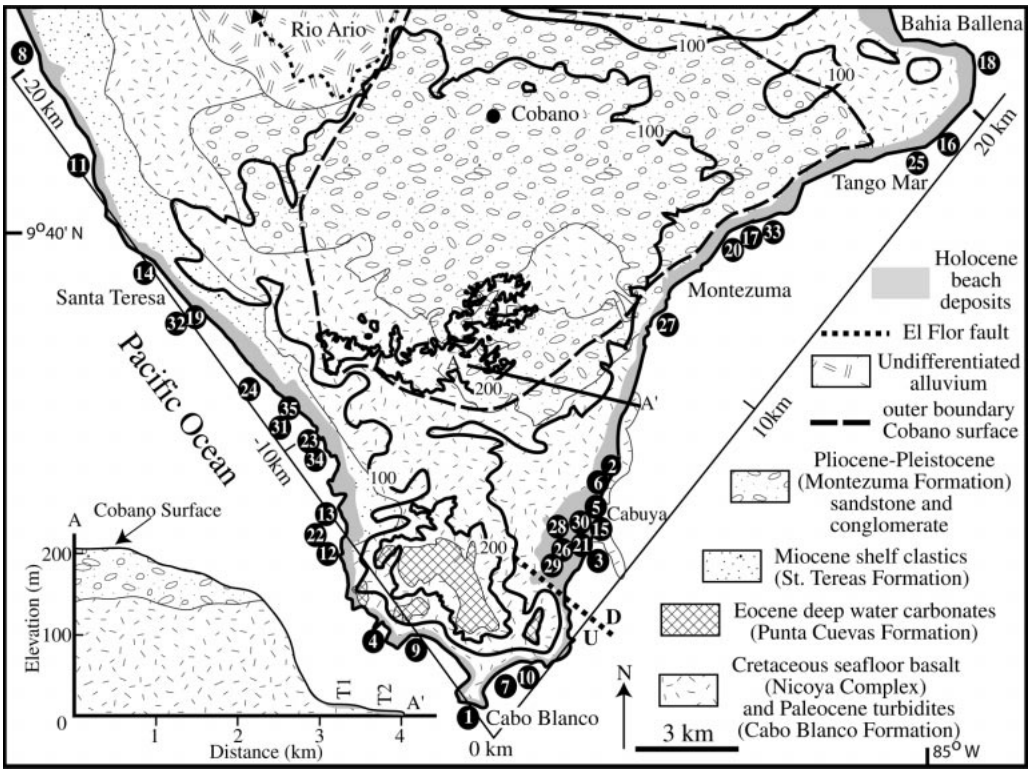

Figure 2. Generalized geology of southeastern tip of Península de Nicoya. Geology is after Mora and Baumgarter (1985), Mora (1985), and Marshall and Anderson (1995). Numbers in black circles are radiocarbon sample locations (see Table 1). Contours for 100 m and 200 m are shown. Line along Pacific and Gulf coasts with distance in kilometers (0 km at Cabo Blanco) is used as x-axis in Figure 3. In cross-section A–A′, T1 and T2 are Holocene terraces.

INTRODUCTION

The Pacific convergent margin of southern Central America provides a superb setting to test the notion that seamount subduction causes forearc deformation. Convergence is nearly orthogonal and exceeds 90 m/k.y. offshore of the Península de Nicoya. Southeastward from the southern tip of the peninsula, the rough bathymetric domain of the Cocos plate subducts northeastward beneath the Caribbean plate and the Panama block at the Middle America Trench (Fig. 1A). Prominent bathymetric features on the rough domain include the aseismic Cocos Ridge, the Quepos Plateau, and the Fisher seamount group (Fig. 1B).

Subduction of these bathymetric features has a profound effect on seismicity (Protti et al., 1995), trench-slope morphology (von Huene and Fluh, 1994; von Huene and Scholl, 1991; Dominquez et al., 1998; von Huene et al., 2000), and the style of both short-wavelength (Marshall and Anderson, 1995; Fisher et al., 1998) and long-wavelength (Gardner et al., 1992) forearc deformation. Tectonic erosion and subsidence of the upper plate margin are considerable. The slope is scalloped and indented around seamounts, and there are large, scarp-bounded depressions where seamounts have penetrated the margin (Fig. 1B). However, 60–100 km inboard of the trench along the subaerial part of the forearc, seamount subduction causes structural segmentation and rapid, differential uplift of fault-bounded blocks (Fisher et al., 1998; Marshall et al., 2000).

Analysis of subaerial forearc deformation in Costa Rica has been limited to one-dimensional, coast-parallel (Fisher et al., 1994, 1998) or coast-perpendicular (Marshall and Anderson, 1995; Gardner et al., 1992) terraces. However, the southeastern tip of the Península de Nicoya with well-preserved, Holocene marine terraces along two perpendicular trending coastlines offers a superb opportunity to determine two-dimensional attributes of deformation related to seamount subduction because it is located ~60 km inboard of the subducting Fisher seamount group on the Cocos plate (Fig. 1B). In this paper we report on the rates, style, and timing of Holocene deformation and further define these results with elevation and dip of the late Quaternary Cobano surface and Pliocene and Pleistocene Montezuma Formation.

HOLOCENE MARINE TERRACES

Two laterally extensive, Holocene marine terraces are well developed along 40 km of nearly perpendicular coastlines at the tip of the peninsula (Fig. 2). The terraces extend nearly 1 km inland and are locally covered with as much as 2 m of fossiliferous, intertidal sands and beach rock. Elevations of terrace inner edges descend systematically along both coastlines away from Cabo Blanco (0 km, Fig. 3A), from a maximum elevation of ~16 m on the upper terrace (T1) and ~5 m on the lower terrace (T2). At a distance of ~20 km from Cabo Blanco along both coastlines, terraces converge to approximately modern mean sea level (Fig. 3A). Locally, each terrace tread exhibits multiple, small (<1 m), laterally discontinuous steps that are not resolvable with radiocarbon dating. They probably indicate short time step (<100 yr), nonlinear, coseismic uplift, which we approximate as a long-term (thousands of years) linear uplift.

UPLIFT RATES AND BLOCK ROTATION

Marine shell samples ($n = 35$) distributed along the entire 40 km coastline (Fig. 2) yield excellent age constraints for both terraces. Ages range from 3.5 to 7.4 ka for terrace 1 and from 0.3 to 2.9 ka for terrace 2 (Table 1). The uplift rate for each dated sample is calculated using the equation:

$$Z\ (\text{m/k.y.}) = \frac{X1\ (\text{m}) + X2\ (\text{m}) + X3\ (\text{m})}{X4\ (\text{ka})}, \quad (1)$$

where Z is uplift rate, $X1$ is modern elevation, $X2$ is facies depth (positive downward from 0 at modern mean sea level), $X3$ is paleo-sea-level depth (positive downward from 0 at modern mean sea level), and $X4$ is calendar calibrated years before 1999. For paleo-sea level we use the most recently refined, composite sea level curve of Fleming et al. (1998).

Maximum uplift rates slightly in excess of 6.0 m/k.y. occur along the southeastern tip of the peninsula at Cabo Blanco, decreasing approximately linearly to <1.0 m/k.y. along the 20 km length of both coastlines (Fig. 3B). Uplift rates for the Holocene terraces approach

TABLE 1. RADIOCARBON SAMPLES LISTED BY AGE WITH ASSOCIATED VALUES USED IN UPLIFT RATE CALCULATIONS

ID (Beta)[§]	Distance[#] (km)	Age[**] (ka)	Modern elevation[††] (m)	Facies depth[§§] (m)	Sea level[##] (m)	Uplift rate[***] (m/k.y.)
Terrace 2						
1 (121769)	−0.3	0.333 (+0.030, −0.030)	2.6	−0.6	0.0	6.0 (3.6-8.9)
2 (121773)	7.1	0.378 (+0.050, −0.110)	2.4	−0.6	0.0	4.8 (2.6-9.3)
3 (032360)*	4.8	0.498 (+0.040, −0.050)	3.4	−1.2	0.0	4.4 (2.8-6.5)
4 (121791)	−3.3	0.588 (+0.025, −0.050)	3.1	−0.6	0.0	4.3 (2.9-5.6)
5 (032361)*	6.3	0.758 (+0.100, −0.060)	3.7	−1.2	0.0	3.3 (2.1-4.6)
6 (121773)	7.0	0.808 (+0.070, −0.100)	4.6	−0.6	0.0	5.0 (3.8-5.2)
7 (121770)	0.8	0.853 (+0.060, −0.090)	5.2	−0.6	0.0	5.4 (4.3-6.9)
8 (131258)	−20.1	0.883 (+0.075, −0.075)	0.9	−1.2	0.0	−0.3 (−1.0-0.5)
9 (121790)	−2.4	0.943 (+0.090, −0.040)	3.5	−1.2	0.0	2.4 (1.5-3.3)
10 (121771)	1.7	1.068 (+0.070, −0.090)	7.2	−1.2	0.5	6.1 (5.1-7.4)
11 (121785)	−16.9	1.103 (+0.070, −0.060)	2.0	−1.2	0.5	1.2 (0.5-1.9)
12 (094100)	−5.6	1.218 (+0.070, −0.070)	4.1	0.0	0.5	3.8 (2.6-5.1)
13 (121788)	−6.7	1.428 (+0.070, −0.100)	2.8	−1.2	0.5	1.5 (1.0-2.0)
14 (121787)	−14.4	1.468 (+0.060, −0.090)	1.8	−0.6	0.5	1.2 (0.7-1.7)
15 (034834)*	5.6	1.533 (+0.050, −0.090)	5.5	0.0	0.5	3.9 (3.0-5.1)
16 (121779)	18.5	1.62 (+0.100, −0.070)	2.3	−0.6	0.5	1.4 (0.9-1.8)
17 (121778)	13.3	1.63 (+0.090, −0.060)	1.7	0.0	0.5	1.3 (0.6-2.2)
18 (121780)	20.9	2.33 (+0.050, −0.150)	3.0	−0.6	1.0	1.5 (1.2-1.8)
19 (121784)	−12.1	2.333 (+0.160, −0.040)	1.2	−0.6	1.0	0.7 (0.4-1.0)
20 (121781)	13.3	2.37 (+0.050, −0.040)	1.3	0.0	1.0	1.0 (0.5-1.5)
21 (032358)*	5.2	2.378 (+0.080, −0.040)	9.5	−0.6	1.0	4.2 (3.7-4.5)
22 (127435)	−6.3	2.918 (+0.090, −0.090)	5.9	0.0	1.2	2.4 (2.0-2.9)
Terrace 1						
23 (121774)	−8.8	3.508 (+0.080, −0.100)	5.8	−0.6	1.5	1.9 (1.7-2.2)
24 (121775)	−10.5	3.748 (+0.080, −0.090)	5.4	0.0	1.5	1.8 (1.5-2.2)
25 (122724)[†]	17.9	4.13 (+0.050, −0.050)	3.9	−1.2	2.0	1.1 (0.7-1.5)
26 (034835)*	5.0	4.338 (+0.090, −0.080)	13.7	0.0	2.0	3.6 (3.0-4.2)
27 (037558)*	11.0	4.563 (+0.100, −0.100)	6.0	−0.6	2.5	1.7 (1.3-2.2)
28 (032359)*	5.3	4.748 (+0.120, −0.170)	16.2	−1.2	2.5	3.7 (3.2-4.2)
29 (036397)*	4.9	5.083 (+0.190, −0.150)	17.1	−0.6	3.0	3.8 (3.4-4.3)
30 (036396)*	5.4	5.273 (+0.060, −0.190)	14.8	−0.6	3.5	3.4 (3.0-3.8)
31 (121776)	−9.2	5.293 (+0.190, −0.150)	5.6	−1.2	3.5	1.5 (1.1-1.9)
32 (121783)	−12.1	5.478 (+0.120, −0.060)	1.1	−1.2	4.5	0.8 (0.5-1.1)
33 (121782)	14.0	6.23 (+0.070, −0.090)	6.2	−1.2	6.0	1.8 (1.5-2.1)
34 (GX25370)	−8.1	7.21 (+0.070, −0.030)	5.5	0.0	7.5	1.8 (1.5-2.1)
35 (117376)	−9.4	7.438 (+0.040, −0.040)	5.8	−1.2	9.0	1.8 (1.6-2.1)

[§] Sample ID as shown in Figure 2 with Beta Analytic number (121774); * indicates samples from Marshall and Anderson (1995); [†] indicates AMS date; GX, Geochron Labs.

[#] Distance along coast from Figure 2.

** Calendar calibrated age and one sigma calibrated error.

[††] Modern elevation from transit surveys (0.01 m error), metric tape (0.01 m error), or altimeter (0.1 m error).

[§§] Facies depth from reconstructed modern environments. Given a tidal range of 2.4 m, facies are assigned to mean sea level, 0.0 m (±1.2 m); swash zone -0.6 m (±0.6 m); or high tide line, -1.2 m (±0.6 m).

[##] Paleo–sea-level from Fleming et al. (1998). Assigned sea-level error is 1 m for samples >4 ka.

*** Uplift rate calculated from equation 1 with maximum and minimum values from accumulated errors listed here. Age calculated from 1999.

zero precisely where major physiographic changes occur along the coast, i.e., at Bahia Ballena, the first large bay along the Golfo de Nicoya coastline and near the mouth of the Río Arío, the first major river along the Pacific (Fig. 2). The largest offset in the linear trend of uplift rate (Fig. 3A, between +7 km and +10 km) has no observable terrace offset along the coast. Neither the elevation data (Fig. 3A) nor the uplift rate data (Fig. 3B) indicate late Holocene activity on the El Flor normal fault (Fig. 2) near the tip of the peninsula (Marshall and Anderson, 1995).

Decreasing uplift occurs along both a margin-perpendicular trend landward from the Middle America Trench, and along a margin-parallel trend away from the axis of the subducting Fisher seamount group (Figs. 1B and 3). Given the nearly orthogonal coastlines and the spatially distributed uplift rates, it is possible to calculate, as a simple three-point problem, the angular rotation rate and rotation direction for this coastal block. The roughly 400 km^2 region along the tip of the peninsula is rotating as a block with an angular rotation rate of ~0.02°/k.y. (northwest side down) about an axis with an azimuth of 80° (Fig. 3B inset).

Rotation of the Holocene terraces is consistent with the gentle, northwest dip of the Cobano surface (2°–3°) and underlying Montezuma Formation (3°–5°). The Cobano surface extends over much of the southern tip of the peninsula, descending from more than 200 m near its southern extent to ~100 m inland from the town of Cobano (Fig. 2). Correlation with radiometrically dated mainland terraces define the age of the Cobano surface to between about 46 and 350 k.y. (Fisher et al., 1998; Marshall, 2000). The Cobano surface probably formed during one or more of the sea-level highstands at oxygen isotope stages 5, 7, or 9 (ca. 80–330 ka). Based on the time-averaged rates of Holocene rotation and uplift, the modern geometry of the Cobano surface can be used to determine the duration of deformation. At Holocene deformation rates the Cobano surface would reach its present attitude and elevation within 100–200 k.y.

DEFORMATION BY SEAMOUNT SUBDUCTION

A reasonable case can be made for seamount subduction as the cause of deformation. The southeastern tip of the Península de Nicoya is ~60 km landward of the Middle America Trench along the trend of the Fisher seamount group (Fig. 1B). Here, the Caribbean plate margin is extensively scalloped (Fig. 1B) within 20 km of the coastline (Dominquez et al., 1998; von Huene et al., 2000). Just oceanward of the tip of the peninsula the Benioff zone occurs at ~12 km depth and the plate boundary exhibits large megalenses that could represent sheared-off seamounts (Ranero and von Huene, 2000). The March 25, 1990, subduction earthquake (Mw = 7.0, depth = 20 km) was located just offshore of Bahia Ballena (Fig. 1B). The arcuate distribution of aftershocks suggests that the rupture was related to seamount subduction (Protti et al., 1995) along the trend of the Fisher seamount group.

Subduction of the Fisher seamount group could reasonably pro-

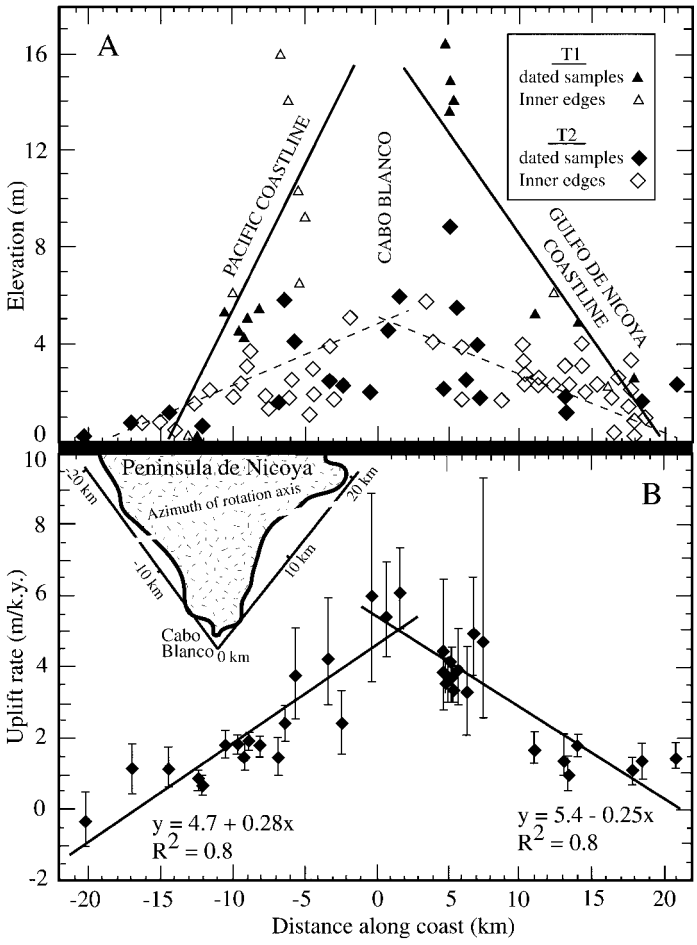

Figure 3. A: Elevation (*X*1 + *X*2, modern elevation plus facies depth to account for facies depth variations among dated samples) vs. distance for all dated samples and additional undated terrace inner edges (paleo-high-tide line) illustrating distinct elevation trends for two terraces along coast. X-axis (distance along coast) for A and B illustrated in B inset is from Figure 2. B: Calculated uplift rate with error bars for all dated samples. Linear best-fit regressions illustrate significant decrease in uplift rates away from tip of peninsula at Cabo Blanco. Thick gray line in inset indicates azimuth direction for block rotation axis; tick is on downdip side.

duce the observed rotation of Holocene terraces along both the margin-parallel and margin-perpendicular coastlines. If this rotation is limited to the past ~200 k.y., as constrained by the geometry of the Cobano surface and Montezuma Formation, then seamounts subducting at the modern convergence rate of ~90 m/k.y. would migrate <20 km along the convergence vector. This distance is similar to the trench-perpendicular length of the deforming block. This length also approximates the length of megalenses (10–15 km; Ranero and von Huene, 2000) imaged at the plate boundary.

Thus, we conclude that the southeastern tip of the Península de Nicoya is uplifting and rotating in response to seamount subduction. The seamount may be underplating onto the Caribbean plate or it may still be subducting. Underplating would produce permanent and cumulative vertical displacement as the line of seamounts subducts. If the seamount remains attached to the Cocos plate, then subsidence may occur after passage of the seamount, as observed along the margin slope (von Huene et al., 2000; Dominquez et al., 1998; Ranero and von Huene, 2000). There is no field evidence to indicate any Quaternary subsidence along the southern tip of the peninsula, suggesting seamount underplating.

CONCLUSIONS

Uplift and rotation of the southeastern tip of the Península de Nicoya are occurring in response to seamount subduction along the projected trend of the Fisher seamount chain. The 35 radiocarbon dates from 2 extensive and well-preserved Holocene marine terraces along 40 km of orthogonal coastline yielded ages ranging from 3.5 to 7.4 ka for an upper terrace and from 0.3 to 2.9 ka for a lower terrace. Uplift rates decrease linearly from a maximum of ~6.0 m/k.y. near the tip of the peninsula at Cabo Blanco to <1.0 m/k.y. along both coastlines. This distribution demonstrates decreasing uplift along both a margin-perpendicular trend landward from the Middle America Trench and along a margin-parallel trend away from the line of subducting seamounts. The 400 km^2 tip of the peninsula is rotating as a discrete block with an angular rotation rate of 0.02°/k.y. about an axis with an azimuth of 80°. Calculated uplift rates are consistent with the elevation of the late Quaternary Cobano surface, the duration of deformation constrained to the past 100–200 k.y. Deformation is occurring in response to seamount bypass or underplating onto the Carribean plate.

ACKNOWLEDGMENTS

This research was partially funded by the William R. Keck Foundation and National Science Foundation grant EAR-95–26955 to Fisher and Gardner. We greatly appreciate the support of Barbara MacGregor, E. Beutner, A. Claypool, E. Hernandez, E. Krall, A. Krull, A. Reeves, T. Shearer, and R. Stamski, and the thoughtful reviews provided by E. Silver, D. Scholl, and J. Webb.

REFERENCES CITED

Barckhausen, U., Ranero, C., von Huene, R., Cande, C., and Roeser, H., 2000, Analogous segmentation of the Cocos plate and the subduction zone off Costa Rica: Institut für Geologie und Palaontologie, Universität Stuttgart, Profil, v. 18, p. 29.

DeMets, G., Gordon, R., Argus, D., and Stein, S., 1990, Current plate motions: Geophysical Journal International, v. 101, p. 425–478.

Dominguez, S., Lallemand, S., Malavieille, J., and von Huene, R., 1998, Upper plate deformations associated with seamount subduction: Tectonophysics, v. 293, p. 207–224.

Fisher, D., Gardner, T., Marshall, J., and Montero, W., 1994, Kinematics associated with late Tertiary and Quaternary deformation in central Costa Rica: Western boundary of the Panama microplate: Geology, v. 22, p. 263–266.

Fisher, D., Gardner, T., Marshall, J., Sak, P., and Protti, M., 1998, The effects of subducting seafloor roughness on forearc kinematics, Pacific coast, Costa Rica: Geology, v. 26, p. 467–470.

Fleming, K., Johnston, P., Zwartz, D., Yokoyama, Y., Lambeck, K., and Chappell, J., 1998, Refining the eustatic sea-level curve since the Last Glacial Maximum using far- and intermediate-field sites: Earth and Planetary Science Letters, v. 163, p. 327–342.

Gardner, T., Verdonck, D., Pinter, N., Slingerland, R., Furlong, K., Bullard, T., and Wells, S., 1992, Quaternary uplift astride the aseismic Cocos Ridge, Pacific coast of Costa Rica: Geological Society of America Bulletin, v. 104, p. 219–232.

Mackay, M., and Moore, G., 1990, Variation in deformation of the south Panama accretionary prism: Response to oblique subduction and trench sediment variation: Tectonics, v. 9, p. 683–698.

Marshall, J., 2000, Active tectonics and Quaternary landscape evolution across the western Panama block, Costa Rica, Central America [Ph.D. thesis]: University Park, Pennsylvania State University, 260 p.

Marshall, J., and Anderson, B., 1995, Quaternary uplift and seismic cycle deformation, Peninsula de Nicoya, Costa Rica: Geological Society of America Bulletin, v. 107, p. 463–473.

Marshall, J., Fisher, D., and Gardner, T., 2000, Central Costa Rica deformed belt: Kinematics of diffuse faulting across the western Panama block: Tectonics, v. 19, p. 468–492.

Meschede, M., Barckhausen, U., and Worm, H., 1998, Extinct spreading on the Cocos Ridge: Terra Nova, v. 10, p. 211–216.

Mora, C., 1985, Sedimentología y geomorfología del sur de la Península de Nicoya (Provincia de Puntarenas, Costa Rica) [Tesis de Licenciatura]: San José, Escuela Centroamericana de Geología, Universidad de Costa Rica, 148 p.

Mora, C., and Baumgarter, P., 1985, Mapa geológico del Sur de la Península de Nicoya: San José, Escuela de Geología, Universidad de Costa Rica, scale 1:50 000.

Protti, M., McNally, K., Pacheco, J., González, V., Montero, C., Segura, J., Brenes, J., Barboza, V., Malavassi, E., Güendel, F., Simila, G., Rojas, D., Velasco, A., Mata, A., and Schillinger, W., 1995, The March 25, 1990 (Mw = 7.0 Ml = 6.8) earthquake at the entrance of the Nicoya Gulf, Costa Rica: Its prior activity, foreshocks, aftershocks and triggered seismicity: Journal of Geophysical Research, v. 100, p. 20,345–20,358.

Ranero, C., and von Huene, R., 2000, Subduction erosion along the middle America convergent margin: Nature, v. 404, p. 748–752.

Silver, E., Reed, D., Tagudin, J., and Heil, D., 1990, Implications of the North and South Panama thrust belts for the origin of the Panama orocline: Tectonics, v. 9, p. 261–281.

von Huene, R., and Scholl, D., 1991, Observations at convergent margins concerning sediment subduction, subduction erosion, and the growth of continental crust: Reviews of Geophysics, v. 29, p. 279–316.

von Huene, R., and Fluh, E., 1994, A review of marine geophysical studies along the Middle America Trench off Costa Rica and the problematic seaward terminus of continental crust: Institut für Geologie und Palaontologie, Universitat Stuttgart, Profil, v. 7, p. 143–159.

von Huene, R., Ranero, C., Weinrebe, W., and Hinz, K., 2000, Quaternary convergent margin tectonics of Costa Rica: Segmentation of the Cocos plate and Central American volcanism: Tectonics, v. 19, p. 314–334.

Manuscript received June 5, 2000
Revised manuscript received October 31, 2000
Manuscript accepted November 5, 2000

Printed in USA